The CXCR4/miR-1910-5p/MMRN2 Axis Is Involved in Corneal Neovascularization by Affecting Vascular Permeability

Xiao Wang,[1,2] Zedu Cui,[1,2] Xi Chen,[1,2] Qian Luo,[1,2] Zihua Jiang,[1,2] Xuan Liu,[1,2] Yuke Huang,[1,2] Jingyi Jiang,[1,2] Shuilian Chen,[1,2] Jin Qiu,[1,2] Yan Li,[1,2] Keming Yu,[1,2] and Jing Zhuang[1,2]

[1]State Key Laboratory of Ophthalmology, Zhongshan Ophthalmic Center, Sun Yat-Sen University, No. 7 Jinsui Road, Tianhe District, Guangzhou, China
[2]Guangdong Provincial Key Laboratory of Ophthalmology and Visual Science, Guangzhou, China

Correspondence: Keming Yu, State Key Laboratory of Ophthalmology, Zhongshan Ophthalmic Center, Sun Yat-Sen University, Guangzhou 510060, China; yukeming@mail.sysu.edu.cn.
Jing Zhuang, State Key Laboratory of Ophthalmology, Zhongshan Ophthalmic Center, Sun Yat-Sen University, Guangzhou 510060, China; zhuangj@mail.sysu.edu.cn.

XW and ZC contributed equally to this work.

Received: January 16, 2023
Accepted: March 18, 2023
Published: April 11, 2023

Citation: Wang X, Cui Z, Chen X, et al. The CXCR4/miR-1910-5p/MMRN2 axis is involved in corneal neovascularization by affecting vascular permeability. *Invest Ophthalmol Vis Sci.* 2023;64(4):10. https://doi.org/10.1167/iovs.64.4.10

Purpose. Chemokine receptor 4 (CXCR4) plays an essential role in the early stage of corneal neovascularization (CNV), but the underlying key molecular mechanism has yet to be addressed. This study aimed to explore the new molecular mechanism of CXCR4 in CNV and the related pathological events.

Methods. CXCR4 was assayed by immunofluorescence or Western blotting. The function of the supernatant from hypoxia-treated human corneal epithelial cells (HCE-T) cells was examined by culturing with human umbilical vein endothelial cells. MicroRNA sequencing was used to detect the downstream microRNAs upon CXCR4 knockdown and analyzed by preliminary bioinformatics. The proangiogenic functions and downstream target genes of microRNA were investigated by gene interference and luciferase assay. An alkali-burned murine model was introduced to examine the function and mechanism of miR-1910-5p in vivo.

Results. High CXCR4 expression was confirmed in corneal tissues of patients with CNV and hypoxic HCE-T cells. The supernatant from hypoxia-treated HCE-T cells is involved in the CXCR4-mediated angiogenesis of human umbilical vein endothelial cells. Notably, miR-1910-5p was demonstrated to be at a high level in wild-type HCE-T cells and its supernatant, and in CNV patient tears. The proangiogenic functions of miR-1910-5p were demonstrated with the assays of cell migration, tube formation, and aortic ring. Moreover, miR-1910-5p significantly inhibited multimerin-2 expression by targeting its 3′ untranslated region and caused significant extracellular junctional defects in human umbilical vein endothelial cells. MiR-1910-5p antagomir could significantly increase multimerin-2 level and decrease vascular leakage, and ultimately inhibit CNV in a murine model.

Conclusions. Our results revealed a novel CXCR4-mediated mechanism and proved that targeting the miR-1910-5p/multimerin-2 pathway could be a promising therapeutic target for CNV.

Keywords: corneal neovascularization (CNV), CXCR4, miR-1910-5p, multimerin-2 (MMRN2)

Corneal neovascularization (CNV) is often caused by a variety of etiologies, such as alkali injury, contact lens wearing, dry eye syndrome, corneal infections, and other ocular surface diseases, which is a major sight-threatening condition worldwide that leads to corneal opacification and even loss of sight.[1,2] CNV originates from preexisting limbal vessels and includes two processes: vasculogenesis and angiogenesis.[3] Moreover, bone marrow–derived circulating endothelial progenitor cells (EPCs) play a key role in vasculogenesis in response to injury,[4] in which EPCs migrate to neovascularization sites and differentiate into endothelial cells (ECs) in situ, a process termed vasculogenesis. Under normal conditions, ECs are stable and interconnected; interendothelial junctions allow only the leakage of small molecules and solutes, thus maintaining tissue homeostasis.[5] Thus, vascular stability and permeability might be damaged during pathological neovascularization. Subsequently, angiogenesis occurs by proliferating ECs and forming new vessels based on preexisting vessels. Despite significant advances in neovascularization studies throughout the decades, treatment of CNV still faces many challenges. The molecular mechanism in the early stage of CNV is not well-defined.

A growing body of literature has reported that CXC motif chemokine receptor 4 (CXCR4), a receptor for SDF-1, is expressed in ECs and EPCs both in vitro and in vivo and plays a major role in the early stages of neovascularization and angiogenesis.[6–8] For example, a study

by Omori et al.[9] demonstrated that SDF-1/CXCR4 interactions might modulate the effects of chronic inflammation and subretinal neovascularization at the retinal pigment epithelial site of the blood–retina barrier. Our previous studies also demonstrated that CXCR4 was significantly upregulated in the corneal epithelium in a model of CNV and was barely expressed in normal corneas.[10,11] Moreover, de Nigris et al.[12] indicated that CXCR4/YY1 transcriptionally regulated VEGF expression and disturbed its network and neovascularization during tumor development. They suggested that CXCR4 might be an upstream target in neovascularization and angiogenesis. Thus, SDF-1/CXCR4 signaling is important in neovascularization and angiogenesis. However, the detailed cellular and molecular mechanisms of CXCR4-mediated signaling in the early stage of CNV remain poorly understood.

Recently, many studies have reported that microRNAs (miRNAs) are small signal transduction molecules involved in neovascular processes.[13,14] The miRNAs are a class of short, highly conserved, noncoding RNAs that bind to target mRNAs to regulate gene expression at the transcriptional and posttranslational levels.[15] Moreover, miRNAs possess the characteristics of high dynamicity and dose sensitivity in quantitative regulation, which serve as generators of graded responses or as signaling amplifiers in regulating distinct cell fates in response to a limited number of signaling cues.[16] In the case of the cornea, miRNAs regulate key pathological conditions of inflammation and neovascularization, such as miR-21, miR-204, and miR-184.[17–19] Wang et al.[20] and Klein et al.[21] demonstrated that miR-7-5p and miR-15a/16-1 might be critical downstream mediators of the CXCL12/CXCR4 axis involved in breast cancer as well as neuroblastoma tumors. However, different miRNAs play a key role in different pathological stages and tissues. The miRNA involved in the early stage of CNV remains poorly explored.

To address these questions, we first confirmed that CXCR4 was highly expressed in the corneas of patients, such as corneal graft rejection, alkaline burns, and corneal leukoma. Human corneal epithelial cells (HCE-T) were treated with hypoxia, which mimics the stimulation in vivo. The supernatant from hypoxia-treated HCE-T cells was confirmed to promote in CXCR4-mediated angiogenesis in vitro. To elucidate the CXCR4-mediated mechanism involved in CNV, tagged miRNA sequencing was performed to obtain the downstream miRNAs of CXCR4 by comparing the knockout cells by CRISPR–Cas9 gene editing technology with normal cells under hypoxic conditions in vitro. Moreover, preliminary bioinformatics was performed to identify miRNAs with significant differences combined with proangiogenic functions. miR-1910-5p was demonstrated to be regulated by CXCR4 and play a crucial role in CXCR4-mediated vascularization for the first time both in vitro and in vivo. Meanwhile, miR-1910-5p was confirmed to be highly expressed in CNV patient tears. More important, the downstream target gene of miR-1910-5p, multimerin-2 (MMRN2), a protein deposited along blood vessels and maintaining vascular homeostasis, was predicted by bioinformatics analysis and verified both in vitro and in vivo. miR-1910-5p antagomir could significantly increase Mmrn2 level and decrease vascular leakage, and ultimately inhibit CNV in a murine model. Thus, to our knowledge, this study revealed a novel mechanism of CXCR4/miR-1910-5p/MMRN2 involved in the early stage of CNV.

Methods

Human Samples

This study was approved by the Ethics Committee of the second affiliated hospital of Guangzhou Medical University (2021-hs-63-02) and informed consent was obtained from all patients before obtaining the samples.

For tear collection, 12 patients and 12 healthy volunteers were enrolled in this study. Twelve healthy volunteers were healthy with no medication or history of ophthalmic disease. Twelve patients were observed having CNV and clinical diagnosis information of patients were summarized in Supplementary Table S1. Basal tears were collected from the external canthus of the inferior fornix using a sterile capillary tube (Seinda Biomedical Corporation, China) according to the manufacturer's protocol. Tears from four different patients or volunteers were pooled as one sample. All tear samples were collected by the same clinician and placed in microtubes and stored at −80 °C until further examination.

Animals and Alkali Burn Injury Model of CNV

All animal experiment procedures in this study were approved by the Institutional Animal Care and Use Committee of Zhongshan Ophthalmic Center (2019-166) and treated for the Use of Animals in Ophthalmic and Vision Research according to the ARVO Statement.

The animal model of alkali burn-induced CNV was established as previously described.[10,22] In brief, a circular piece of filter paper (2.0 mm in diameter) soaked with 1 M NaOH was placed on the surface of the cornea for 40 seconds by a surgical microscope. After alkali exposure, the ocular surface was then rinsed with 0.9% saline (10 mL). The slit-lamp biomicroscope examination was monitored daily to observe the development of CNV. One day after the alkali injury, mice were divided randomly into three groups. Ten microliters of miR-1910-5p antagomirs (2.5 nmol, Tsingke Biotechnology, Beijing, China), antagomir negative control (antagomir control, 2.5 nmol), or PBS was injected into the subconjunctival space at 2 and 8 days after injury. CNV was observed by an ophthalmologist and photographed under the fluorescence microscope (Nikon Eclipse Ni-U) on day 10 after the operation.

Cell Culture and Treatment

The HCE-T cell was kindly provided by Prof. Wu of Sun Yat-Sen University. HCE-T cells were cultured in DMEM/F12 containing 10% fetal bovine serum, 5 µg/mL insulin, and 5 µg/mL epidermal growth factor. The human umbilical vein ECs (HUVECs) were purchased from the ATCC Collection (Manassas, VA, USA) and cultured in EC medium supplemented with 5% of fetal bovine serum, 1% P/S, and 1% ECGS. All cells were cultured in a humidified atmosphere at 37 °C.

The corneal epithelial chronic injury process was imitated by the model of hypoxic stimulation of the HCE-T cells in vitro by culturing in the mixing of 5% CO_2, 1% O_2, and 94% N_2 at 37 °C in a humidified atmosphere for 48 hours.

Cell transfection were performed using Lipofectamine 3000 (Invitrogen, Waltham, MA, USA) at a final concentration of 50 nM (miRNA mimic or mimic control) and 100 nM (miRNA inhibitor or inhibitor control) following the manufacturer's instructions (Tsingke Biotechnology).

Cell Viability Assay

The effect of CXCR4 knockout and miR-1910-5p overexpression on the viability of cell proliferation was determined using the CCK-8 assay (Dojindo Laboratories, Kumamoto, Japan) following the manufacturer's instructions. The absorbance was measured at 450 nm followed by incubation with CCK-8 reagent for 3 hours at 37 °C.

RNA Extraction and Quantitative PCR (qPCR)

Total RNA was extracted with TRIzol reagent (Thermo Fisher Scientific, Waltham, MA USA) and cDNA was synthesized using a PrimeScript RT Reagent kit (Takara, Shiga, Japan). For the patients' tears RNA extraction, TRIzol reagent and Dr. GenTLE precipitation carrier (Takara) were used. RNA was reverse transcribed into mature miRNA using the Mir-X miRNA First-Strand Synthesis Kit (Takara). The expression levels of mRNA and miRNAs were measured by qPCR using SYBR PrimeScript RT-PCR kit (Takara). β-Actin and U6 were used as an internal control for mRNA and miRNA detection, respectively. The primers are listed in Supplementary Table S2. The reverse primer of miRNAs was provided by The Mir-X miRNA First-Strand Synthesis Kit.

Small RNA Sequencing and Sequencing Data Analysis

Total RNA from wild-type (WT) cells and CXCR4-knocout (KO) cells in the presence of hypoxia for 48 hours was isolated using TRIzol reagent. Three qualified biological replicates of each sample were sequenced. One microgram of total RNA was used to prepare a small RNA library, according to the protocol of TruSeq Small RNA Sample Prep Kits (Illumina, San Diego, CA, USA). Libraries were sequenced by Illumina Hiseq 2000/2500 (Illumina) with single-end 50-bp read length. Raw reads were subjected to an in-house program, ACGT101-miR (LC Sciences, Houston, TX, USA) to remove adapter dimers, junk, low complexity, common RNA families (ribosomal RNA, transfer RNA, small nuclear RNA, small nucleolar RNA), and repeats. Subsequently, unique sequences with length in 18 to 26 nucleotides were mapped to specific-species precursors in miRBase 22.0 by BLAST search to identify known miRNAs and novel 3p- and 5p-derived miRNAs. Differential expression of miRNAs based on normalized deep sequencing counts was analyzed using the Student *t*-test. The significance threshold was set at a P value of <0.05. All sequencing data have been uploaded to GEO (GSE226185).

Western Blot Assay

Cells and cornea tissue proteins were extracted with RIPA extraction buffer completed with protease inhibitors. Ten micrograms of total protein per sample were loaded into SDS-PAGE gels and transferred to PVDF membranes, then blocked with 5% milk at room temperature (RT) for 3 hours. The membranes were incubated with primary antibodies overnight at 4° (Supplementary Table S3). The membranes were further incubated with anti-rabbit secondary antibody (cat no: 7074, CST) or anti-mouse secondary antibody (cat no: 7076, CST) for 2 hours at RT. The band intensity was quantified using Image J software.

Immunofluorescence Staining Assay

HCE-T cells, HUVECs, and aortic ring tissues were fixed with 4% paraformaldehyde for 1 hour and blocked with 5% BSA with the addition of 0.3% Triton X-100 for 30 minutes, then incubated overnight at 4 °C with primary antibodies (Supplementary Table S3). Alexa Fluor 555 anti-rabbit lgG (cat no: 4413, CST) and Alexa Fluor 488 anti-mouse lgG (cat no: 4408, CST) were served as secondary antibodies. Images were captured using fluorescence microscopy (Zeiss, Jena, Germany). The mean fluorescence intensity was evaluated by the ImageJ software.

Immunofluorescence for an EC marker (CD31) was performed on whole cornea tissues to assess CNV lesion size as previously described.[10,22] Briefly, mice were euthanized and corneas were fixed in 4% paraformaldehyde for 1 hours at RT. Then corneas were treated with 0.3% Triton and 5% BSA blocking buffer for 2 hours, then incubated in primary antibody CD31 (cat. no: 553370, BD Pharmingen, Franklin Lakes, NJ, USA) for 16 hours at 4 °C and in Alexa Fluor 488 Goat anti-Rat IgG (H+L) antibody (cat. no: A-11006, Invitrogen) for 3 hours at RT. All corneas were carefully dissected radially into four pie-shaped wedges and then flat-mounted. The vessels were visualized using a fluorescence microscope. The CD31-positive fluorescent areas of corneas were evaluated with Image J software.

Wound Healing Assay and Tube Formation Assay

HUVECs were seeded on six-well plates and cultivated at 37 °C. On reaching 90% cell confluence, the medium was exchanged to serum-free EC medium. A-200 µL pipette was used to make scratches when the cell density was 100%. Meanwhile, the cell culture medium was replaced by conditioned medium (CM, supernatant of HCE-T cells and a fresh culture medium, 1:1 by volume). The picture was captured at specific time points. The scratch area was determined by a light microscope and analyzed by Image J software.

For tube formation assay, the 96-well plates were precoated with 50 µL/well Matrigel and allowed to solidify at 37 °C for 30 minutes. Then, HUVECs were gently seeded on top of the Matrigel in the presence of a supernatant of HCE-T cells together with a fresh medium 1:1 ratio. The formation of the capillary-like structure after 3 hours was captured using a light microscope. The average number of nodes, junctions, and meshes was calculated from three fields in each sample by using Image J software.

Aortic Ring Assay

Aortic ring assays were prepared by modification of the protocol. Briefly, the thoracic aorta was dissected from C57/BL6J mice, placed in ice-cold DMEM medium, and cut into several aortic rings (0.5 mm thick). Aortic rings were serum-starved and transfected with 100 nM miR-1910-5p mimic and mimic control using Lipofectamine 3000 for 24 hours and then embedded in Matrigel (10 mg/mL). The capillary sprouts of aortic rings were monitored every day for up to 9 days. The area of the outer aortic vessel sprouting was quantified by using the Image J software.

Luciferase Reporter Assay

The promoter sequence of miR-1910-5p (host gene: C16orf74, −2589 bp to +529 bp) was inserted into pGL3

Investigative Ophthalmology & Visual Science

basic reporter vectors (Promega, Madison, WI, USA). HCE-T cells were transfected with miR-1910-5p-Luc and CXCR4/control vectors using Lipofectamine 3000.

For the miRNA luciferase reporter assay, the full-length 3′-untralnslated region (UTR) sequence of MMRN2 was amplified and cloned into the pMIR-REPORT luciferase vector. The luciferase reporter plasmids (pMIR-WT or pMIR-mutant recombinant vector) were simultaneously transfected with miR-1910-5p mimics/mimic controls or inhibitors/inhibitor controls into cultured HCE-T cells using Lipofectamine 3000. At 48 hours after transfection, luciferase activity was measured using the Dual-luciferase Reporter Assay system (cat no: E1960, Promega).

Visualization of Leakage of Corneal Vessels

The 2000-kDa FITC–dextran (50 mg/mL, 250 µL, Sigma-Aldrich, St. Louis, MO, USA) was injected into the tail veins of miR-1910-5p antagomir or antagomir control or PBS-treated C57/BL6J mice at 10 days after alkali burn. After the FITC–dextran had circulated for 10 minutes, the mice were sacrificed and the eyes were enucleated. The corneas were fixed for 30 minutes in 100% acetone, flat-mounted corneas were performed as described earlier and examined by fluorescence microscope. Similarly, ImageJ software was performed to determine the fluorescent area.

Statistics

All data are expressed as the mean ± SD. Differences between two groups were assessed using a two-tailed Student *t*-test. Differences among more than two groups were assessed by one-way ANOVA. Each experiment was repeated at least three times. A P value of <0.05 was required for results to be considered statistically significant.

Results

CXCR4 Is Significantly Upregulated in Corneal Epithelial Tissue of Patients With CNV

In our previous study, CXCR4 was upregulated dramatically in the neovascularized cornea in an animal model of corneal burns after alkali exposure compared to in the healthy cornea.[10] Here, we first identified CXCR4 expression in primary human neovascularized corneal tissue of common corneal neovascular diseases, including corneal graft rejection, alkaline burns, and corneal leukoma.

As shown in Figure 1, CXCR4 expression was barely detectable in normal patients. In contrast, in corneal epithelium from patients with CNV, CXCR4 expression was markedly upregulated in the cytoplasm (white arrowhead), cell membrane (white triangle), and nucleus (yellow arrowhead). These results clinically indicate that CXCR4 is involved in the process of CNV.

CXCR4 Is Highly Expressed in Hypoxic HCE-T Cells, and CXCR4 Knockout Reduces Proangiogenic Activity of CM From Hypoxic HCE-T Cells

To explore the potential molecular mechanism of CXCR4 in CNV, we first used an in vitro model of HCE-T cells subjected to hypoxia damage by exposing HCE-T cells to 1% O_2 for 48 hours. As indicated in Figure 2A, Western blotting assay showed hypoxia-inducible factor and CXCR4 were significantly upregulated in response to 1% O_2 compared with normoxic conditions. The relative intensities of CXCR4 were quantified by densitometry and normalized to β-tubulin levels. Meanwhile, an immunofluorescence staining assay also exhibited that CXCR4 expression was upregulated in HCE-T cells treated with hypoxia (Fig. 2B).

To further investigate the molecular functions of CXCR4 in angiogenesis, we knocked out CXCR4 in HCE-T cell lines using the CRISPR–Cas9 system. The single guide RNA recognition position was designed in the second exon (Fig. 2C). To guarantee CRISPR–Cas9 knockout efficiency, we selected three candidate single clones with similar target single guide RNA recognition positions. The sequencing result of a Sg-CXCR4 clone (Fig. 2D) indicated that a two-base deletion was produced by the CRISPR–Cas9 system, which led to a frameshift in the CXCR4 gene. Immunofluorescence staining and Western blotting assays confirmed it (Figs. 2E, F). Then, the impact of CXCR4 knockout on cell proliferation was detected by CCK8 assay. Our data indicated that cell proliferation was significantly inhibited in the CXCR4−KO group compared with the control group (Fig. 2G).

Owing to the supernatant of hypoxic cells playing a pivotal role in signal transduction, the influence of CM from CXCR4-KO or WT cells under hypoxic conditions was examined. As shown in Figures 3A and B, there was no difference in the cell migration rate at 24 hours, but there was a significant decrease in the HUVEC migration rate at 48 hours after treatment with CM from CXCR4-KO cells compared with that treatment with CM from WT cells. Accordingly, tube formation assays indicated that the average number of nodes, junctions, and meshes formed by HUVECs treated with the CM from CXCR4-KO HCE-T cells significantly decreased compared with those of the controls (Figs. 3C, D). Overall, these results indicate that the CM from CXCR4-KO cells cannot support HUVEC migration and angiogenesis. Moreover, the alternative material in the supernatant plays a key role in the migration and angiogenesis of HUVECs in vitro.

Identification of miR-1910-5p as a Target miRNA Regulated by CXCR4 Under Hypoxia Impairment

MiRNAs are mainly deposited in the CM to deliver signals to other cells.[16] Thus, tagged miRNA sequencing was performed to compare the expression patterns of miRNA between WT HCE-T and CXCR4-KO cells under hypoxic conditions. Among the significantly changed miRNAs, three miRNAs were upregulated and 33 miRNAs were downregulated during CXCR4 knockout (Supplementary Table S4). Then, we screened 14 differentially expressed miRNAs that were downregulated by 2-fold (log2) in CXCR4-KO cells compared with WT cells (Fig. 4A). Gene Ontology enrichment analysis indicated that targeted genes for total differential miRNAs were involved in angiogenic processes (Fig. 4B). To identify angiogenesis processes regulated by a certain miRNA, we confirmed that three miRNAs (miR-1224-5p, miR-10526-3p, and miR-1910-5p) were closely related to the angiogenesis process. The following qPCR assays also identified that miR-1910-5p was significantly decreased in CXCR4-KO cells compared to in WT cells (Fig. 4C). Moreover, miR-1910-5p was significantly upregulated in hypoxic HCE-T cells compared with the control (Supplementary Fig. S1). More important, miR-1910-5p was significantly higher in the

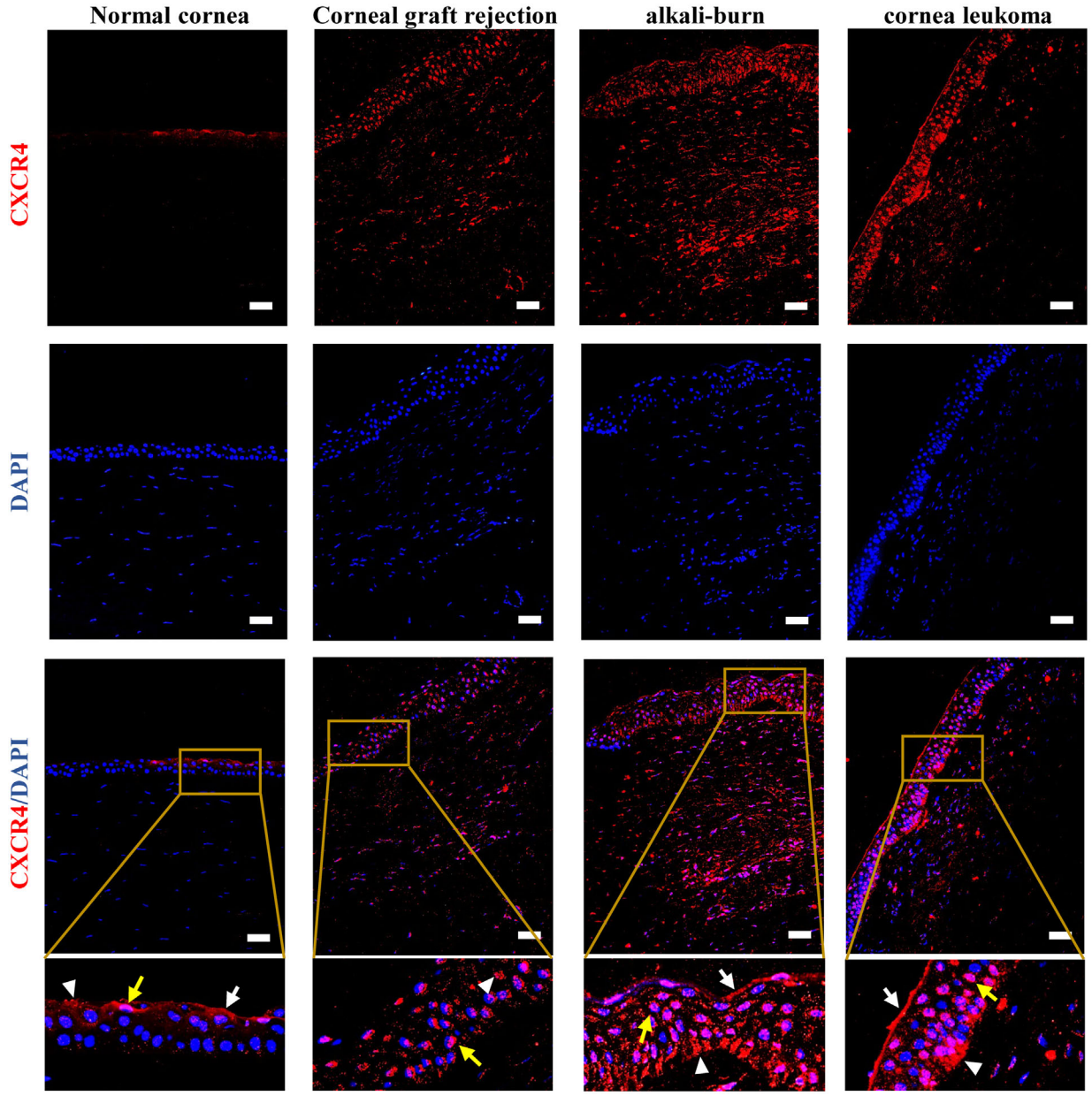

Figure 1. CXCR4 is significantly upregulated in the corneal epithelial tissue of patients with CNV. Immunofluorescence staining of CXCR4 was highly expressed in neovascularized corneas of corneal graft rejection (48 years old, female), alkaline burns (33 years old, male) and corneal leukoma (45 years old, male). Scale bars, 200 µm. The *yellow arrowhead* indicates nuclear staining, the *white arrowhead* indicates cytoplasmic staining, and the *white triangle* indicates cell membrane staining.

tear samples of patients with CNV than in the normal tears (Figs. 4D, E). This abnormal evidence was not observed for miR-1224-5p and miR-10526-3p (data not shown). Notably, to date, few papers have reported that miR-1910-5p is expressed in some cells and tissues.[23–26] There is no study on its proangiogenic and other functions.

Based on the high expression of miR-1910-5p in tears and angiogenic-associated properties of CM from HCE-T cells, the supernatants of HCE-T cells were collected and assayed for miR-1910-5p expression level. Consistent with our speculation, miR-1910-5p was significantly higher in supernatant of hypoxia-treated HCE-T cells than normoxia-treated cells. Accordingly, knockout of CXCR4 significantly decreased miR-1910-5p expression levels in the supernatant of CXCR4-KO cells compared with the WT cells (Fig. 4F). Thus, we focused on the mechanism and bioactivity of miR-1910-5p in subsequent experiments.

CXCR4 Transcriptionally Regulates miR-1910-5p Expression

To reveal whether CXCR4 transcriptionally regulated miR-1910-5p, HCE-T cells were transfected with a plasmid expressing CXCR4 (CXCR4-OE) and a vector (control). The relative intensities of CXCR4 were quantified by densitometry and normalized to β-tubulin levels (Fig. 5A). Then, the miR-1910-5p expression level was

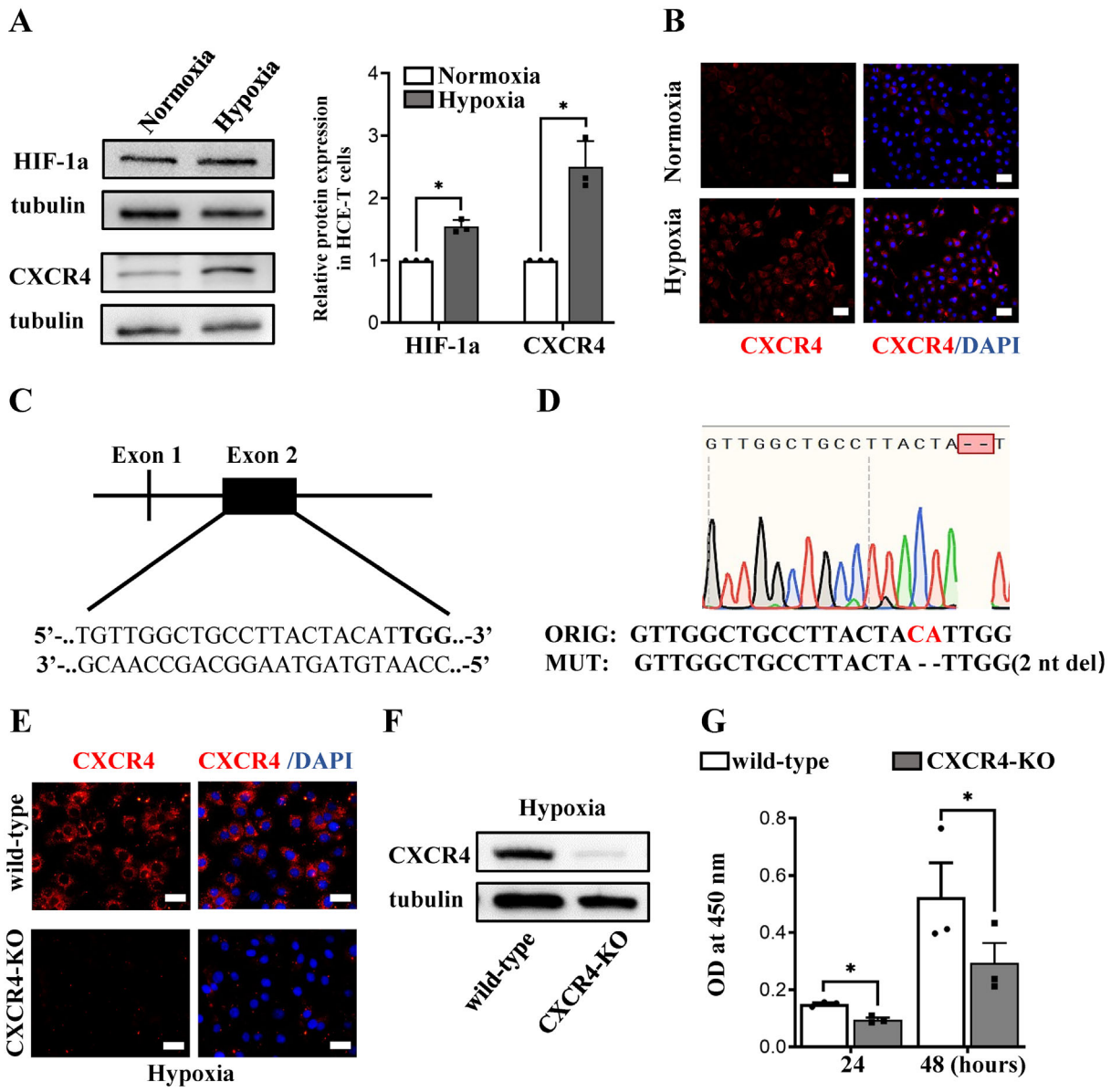

Figure 2. CXCR4 is highly expressed in hypoxic human corneal epithelial (HCE-T) cells, and establishes stable cell lines with a single knockout of the CXCR4 gene in HCE-T cells. (**A**, **B**) Hypoxia-inducible factor-1a and CXCR4 were highly expressed in HCE-T cells under hypoxic conditions compared to normoxic conditions according to Western blotting (**A**) and immunofluorescence assays (**B**). The relative protein expression was quantified using ImageJ software. Scale bars, 100 µm. (**C**) The knockout target sequence of CXCR4 is located in exon 2. The single guide RNA (sgRNA) sequence is shown in *black*. The protospacer adjacent motif (PAM) sequence is indicated in *bold type*. (**D**) In HCE-T cells, after transfection with CRISPR–Cas9 vector lentivirus, the PCR products of CXCR4 gene knockout (CXCR4-KO) monoclonal cells were sequenced. (**E**) An immunofluorescence staining assay was used to detect the expression of CXCR4-KO monoclonal cells. Scale bars, 100 µm. (**F**) Western blotting was used to detect the expression of CXCR4 in CXCR4-KO monoclonal cells. (**G**) CCK-8 assay indicated that the knockout of CXCR4 represses HCE-T-cell proliferation. Data are presented as the means ± SD ($n = 3$). *$P < 0.05$. The Student *t*-test was used for comparison.

assayed by qPCR. As shown in Figure 5B, the overexpression of CXCR4 resulted in upregulation of miR-1910-5p in HCE-T cells. Because hsa-miR-1910-5p is located within a noncoding transcript of C16of74 on chromosome 16 and is cotranscribed with this host gene, C16orf74, was analyzed as a control (https://www.ncbi.nlm.nih.gov/). Similarly, C16orf74 was increased in CXCR4-OE cells compared with control cells. In contrast, CXCR4 knockout also decreased the levels of C16orf74 in HCE-T cells compared with in the control cells (Fig. 5C). Thus, these results indicated that CXCR4 could affect the transcription of miR-1910-5p.

Notably, proteins with transcriptional regulation roles, such as transcription factors, typically have nuclear-localized or nuclear translocation. Previous studies have also demonstrated that nuclear CXCR4 expression has been observed in several malignment tumors, such as breast cancer,[27] colorectal cancer,[28] and thyroid carcinoma.[29] Therefore, we speculate that similar nuclear translocation occurs in HCE-T cells upon pathological stimulation. As expected, CXCR4

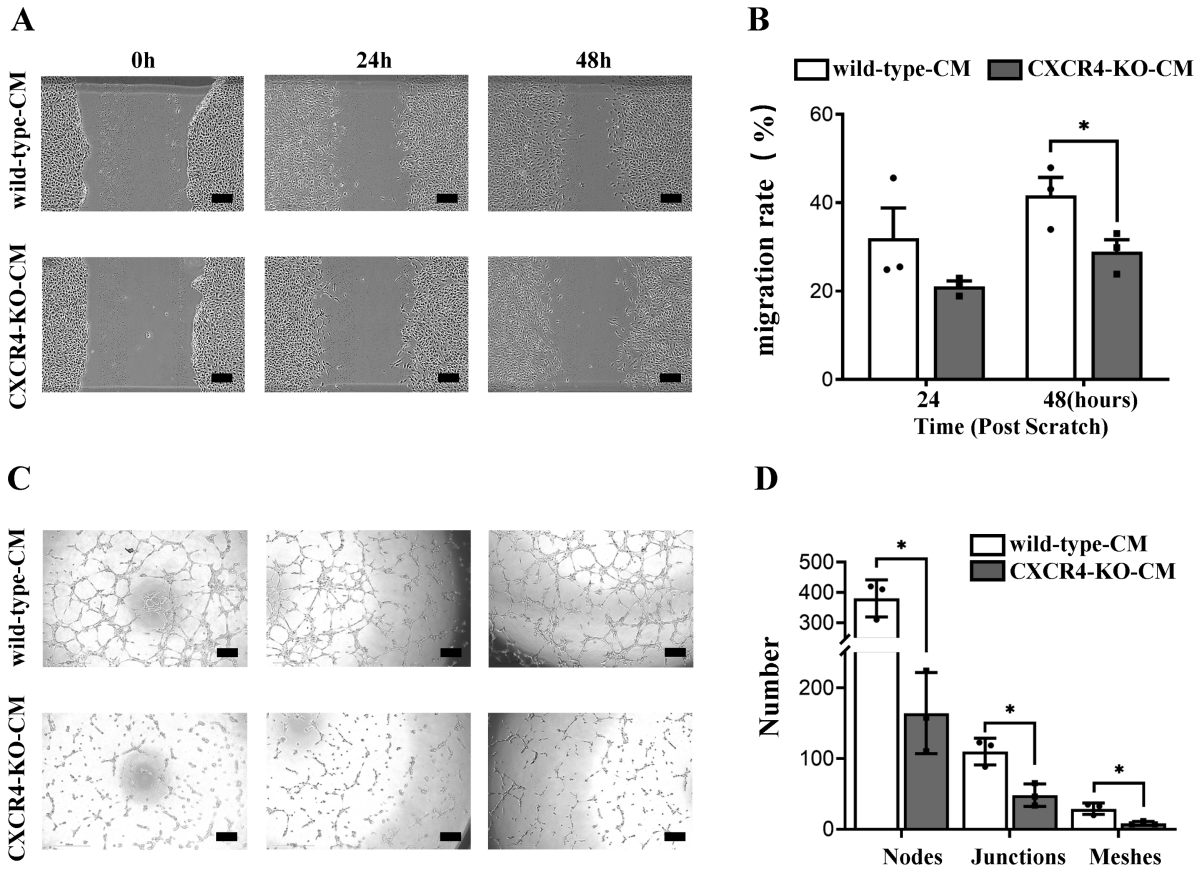

Figure 3. CXCR4 knockout alleviates proangiogenic activity of CM from hypoxic HCE-T cells. (**A**, **B**) Representative images and histogram showing the migration rate at the indicated time points during the wound healing assay. (**C**, **D**) Representative images and quantitative analysis of tube formation characterized the number of nodes, junctions and meshes. Scale bar, 100 µm. Data are presented as the means ± SD ($n = 3$). *$P < 0.05$. The Student *t*-test was used for comparison.

was mostly localized to the cytoplasm of normoxic corneal epithelial cells (Fig. 5D, top), and upon hypoxia treatment for 48 hours, the nuclear translocation of CXCR4 was observed by positive nuclear immunostaining (Figs. 5D, E). Then, we examined the expression location of CXCR4 by extracting nuclear and cytoplasmic proteins by Western blotting assay. As shown in Figures 5F and G, CXCR4 was expressed in the cytoplasm and obviously in the nucleus under hypoxia treatment. The relative intensities of the bands were quantified by densitometry and normalized to the levels of β-tubulin (cytoplasm) or Lamin A+C (nuclear). These results implied that CXCR4 might enter the nucleus and perform an upstream transcriptional activation role to regulate the expression of miR-1910-5p. Hypoxia-inducible factor-1a was a relative reference.

MiR-1910-5p Promotes HUVECs Migration, Tube Formation and Proliferation, and Increases Angiogenesis in Aortic Rings

CXCR4 knockout might induce many changes in the expression profile. Does miR-1910-5p play a key role in the proangiogenic process? To directly confirm the proangiogenic effects of miR-1910-5p, the miR-1910-5p mimic and inhibitor and its controls were transfected into HUVECs. As shown in Figures 6A and B, the miR-1910-5p mimic significantly promoted cell migration after transfection for 24 hours compared with the mimic control; in contrast, the miR-1910-5p inhibitor significantly suppressed the migration of HUVECs compared with the controls. In addition, the miR-1910-5p mimic substantially promoted tube formation of HUVECs, resulting in an increase in the number of nodes, junctions, and meshes. In contrast, the miR-1910-5p inhibitor significantly suppressed tube formation, resulting in the reduction of nodes, junctions, and meshes in HUVECs (Figs. 6C, D).

Moreover, we evaluated the influence of miR-1910-5p on angiogenesis phenotype by culturing mouse aortic rings transfected with miR-1910-5p mimics or the mimic controls (Fig. 6E). From days 4, 6, and 9 after aortic ring explantation, there was a significantly larger sprouting area (red arrow) in aortic rings treated with the miR-1910-5p mimic compared with the controls. Consequently, miR-1910-5p could promote angiogenic sprouting in vitro. Similarly, miR-1910-5p significantly increased cell proliferation compared to the control at 48 and 72 hours after treatment (Fig. 6F). Collectively, these results provide direct evidences to support that miR-1910-5p promoted angiogenesis in vitro.

miR–1910–5p Acts as a Novel Upstream Regulator of MMRN2, a Protein Maintaining Vascular Homeostasis, by Directly Targeting Its 3′-UTR

To further elucidate miR–1910–5p–mediated downstream genes, four different prediction algorithms (miRWalK, miRDB, TargetScan, and miRanda) were used to predict

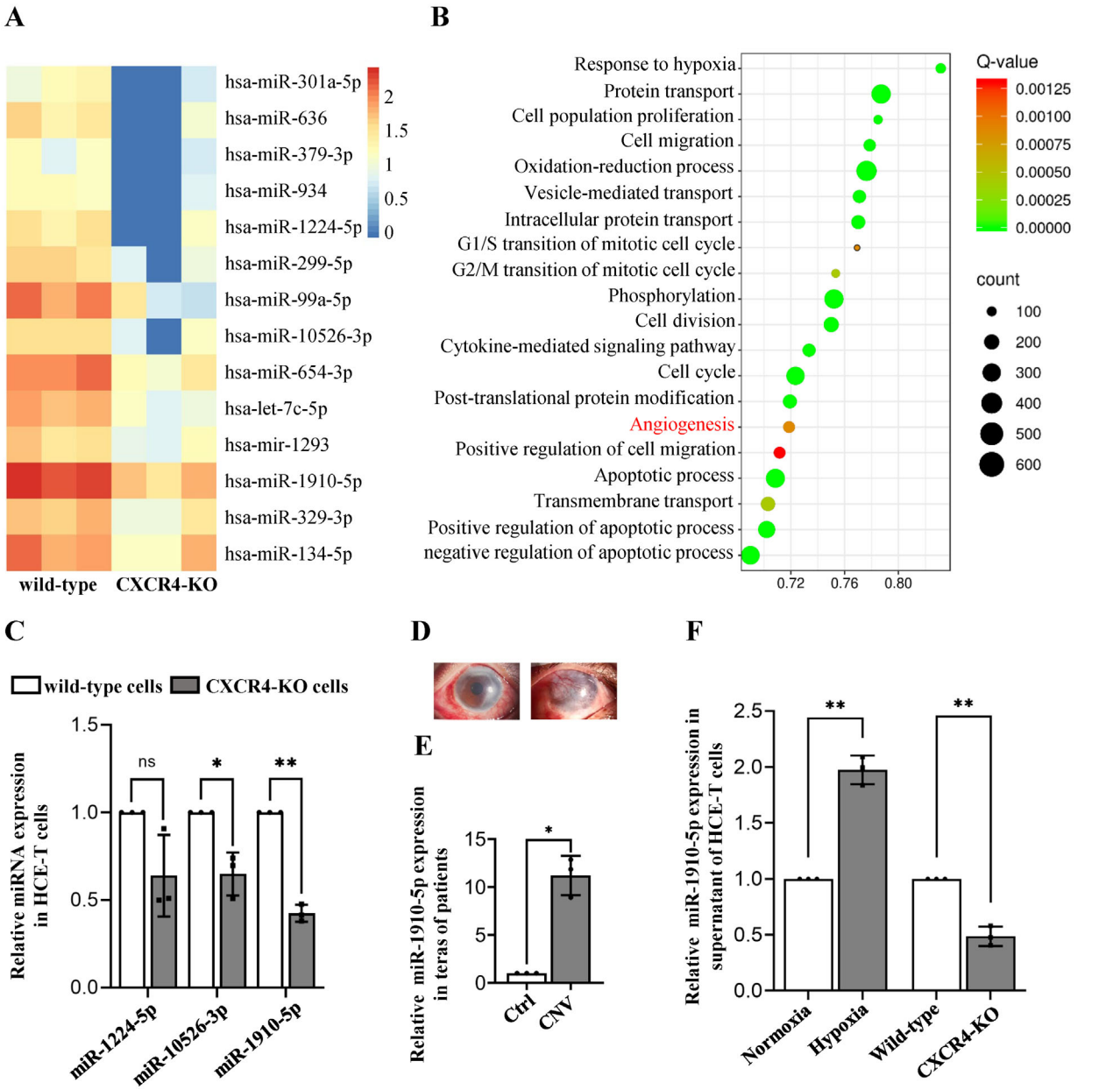

Figure 4. Identification of miR-1910-5p as a target miRNA regulated by CXCR4 under hypoxia impairment. (**A**) Heatmap of the differential expression levels of miRNAs in WT and CXCR4-KO cells under hypoxic conditions. In the heatmap, each row represents a single miRNA, and each column represents an individual sample. The color scale shown on the right illustrates the expression level (log2) of a miRNA across all samples. Each column represents the average of three biological replicates. The relatively high expression is indicated in red, whereas the relatively low expression is indicated in blue. (**B**) Gene Ontology (GO) analysis indicated the target genes of differentially expressed miRNAs in various processes. (**C**) The expression levels of three differential miRNAs from tagged miRNA sequencing were validated by qPCR. (**D**, **E**) Representative clinical photographs of patients with CNV are shown. The qPCR analysis results showed that the relative expression of miR-1910-5p in the tear fluid of patients with CNV was significantly higher than that in the control group. (**F**) miR-1910-5p showed higher expression in hypoxic HCE-T cells than normoxia group, and downregulated in CXCR-KO cells under hypoxic stimulation compared with WT cells. Data are presented as the mean ± SD ($n = 3$). *$P < 0.05$, **$P < 0.01$. The Student t-test was used for comparison.

miR-1910-5p target genes. One hundred twenty-six genes were identified as the most likely downstream targets of miR-1910-5p (Fig. 7A). Because miRNAs mainly inhibit target genes at the posttranscriptional level, the negative regulation of angiogenic genes regulated by miR-1910-5p was our candidate of interest. The selected 126 overlapping genes were then deposited into the Database for Annotation, Visualization and Integrated Discovery for further Gene Ontology enrichment analysis. The results indicated that there were three antiangiogenic genes (VASH1, ISM1, and MMRN2) for the next screening step (Fig. 7B). The TargetScan algorithm showed that the bases from 2947 to 2953, 680 to 686, and 189 to 195 in the VASH1, ISM1, and MMRN2 3′-UTRs have perfect complementarity to the seed sequence of miR-1910-5p, respectively (Fig. 7C, Supplementary Fig. S2). The qPCR results exhibited that the miR-1910-5p mimic significantly decreased the expression of VAH1, ISM1, and MMRN2 (Supplementary Fig. S3).

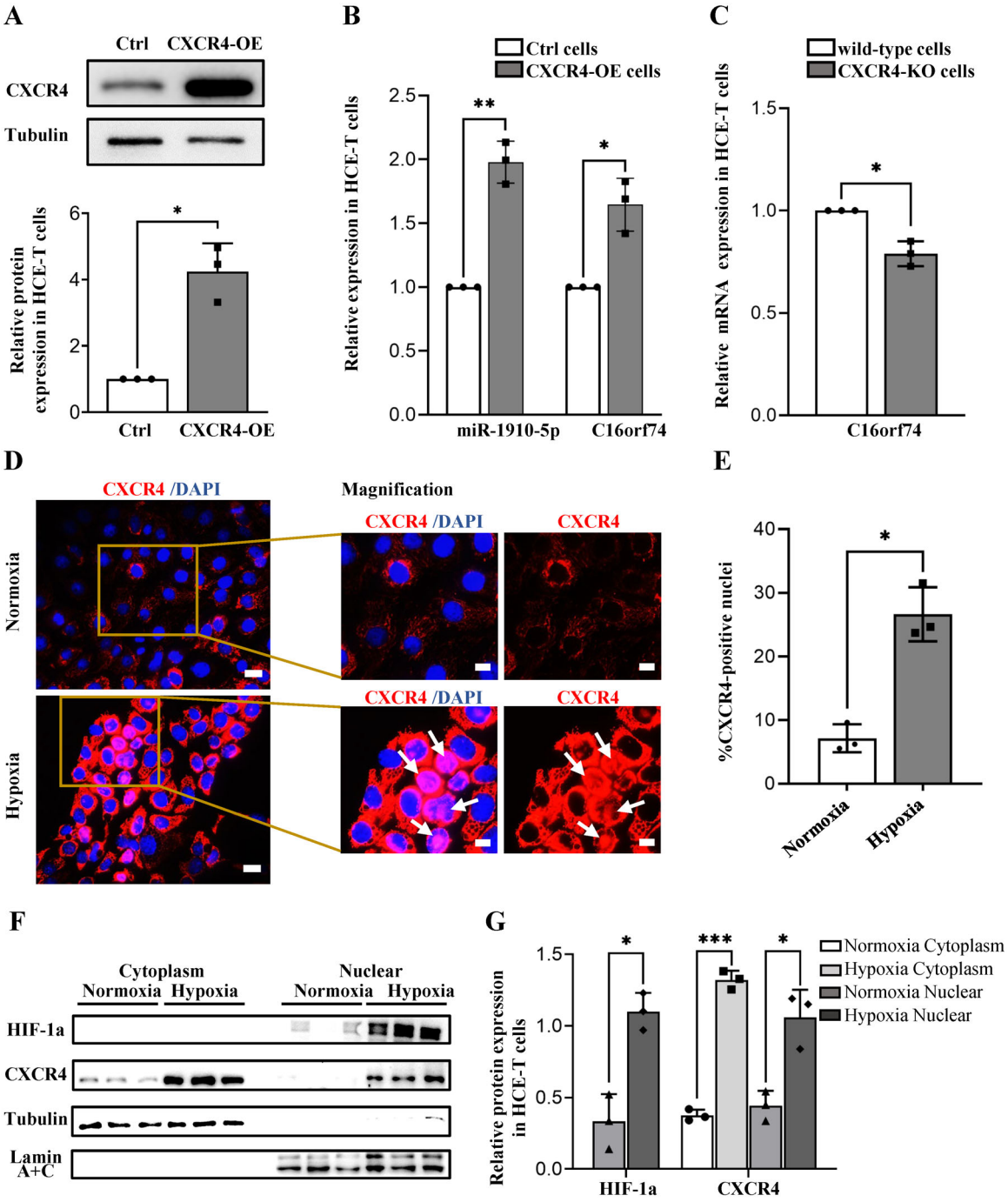

Figure 5. CXCR4 transcriptionally regulates miR-1910-5p expression. (**A**) After transfection of CXCR4-overexpressing plasmid, CXCR4 protein expression levels were significantly upregulated in HCE-T cells. (**B**) miR-1910-5p and C16orf74 showed higher expression in CXCR4-overexpressing (CXCR4-OE) HCE-T cells than in control cells. (**C**) Conversely, C16orf74 showed lower expression in CXCR4-KO cells under hypoxia treatment than in the WT cells. (**D**) Immunofluorescence analysis of CXCR4 cytoplasm and nuclear localization in HCE-T cells. *Arrowheads* indicate the nuclear localization of CXCR4. (**E**) The percentage of CXCR4-positive nuclei (%) in the HCE-T cells was quantified. (**F**, **G**) Western blot analysis of CXCR4 and hypoxia-inducible factor-1α in the subcellular fractions of HCE-T cells treated with hypoxia for 24 hours. Tubulin and Lamin A+C were used as the cytoplasmic and nuclear markers, respectively. Data are presented as the means ± SD ($n = 3$). $^{*}P < 0.05$, $^{**}P < 0.01$, $^{***}P < 0.001$. The Student *t*-test was used for comparison.

To substantiate the site-specific repression of miR-1910-5p on target genes, we constructed WT and mutant VASH1, ISM1, and MMRN2 3′-UTR luciferase reporters. Luciferase activity assays showed that the WT MMRN2 3′-UTR constructs were significantly inhibited by the miR-1910-5p mimic, whereas it was not altered in mutant MMRN2 3′-UTR constructs (Fig. 7D). Conversely, the miR-1910-5p inhibitor significantly enhanced the luciferase activity of the WT MMRN2 3′-UTR, not in the mutant construct of the MMRN2 3′-UTR (Fig. 7E). For the other two genes (VASH1 and ISM1), the miR-1910-5p mimic did not change the luciferase activity of the WT or mutant construct of the 3′-UTR (data not shown). Thus, only MMRN2 was supposed to be a target of miR-1910-5p.

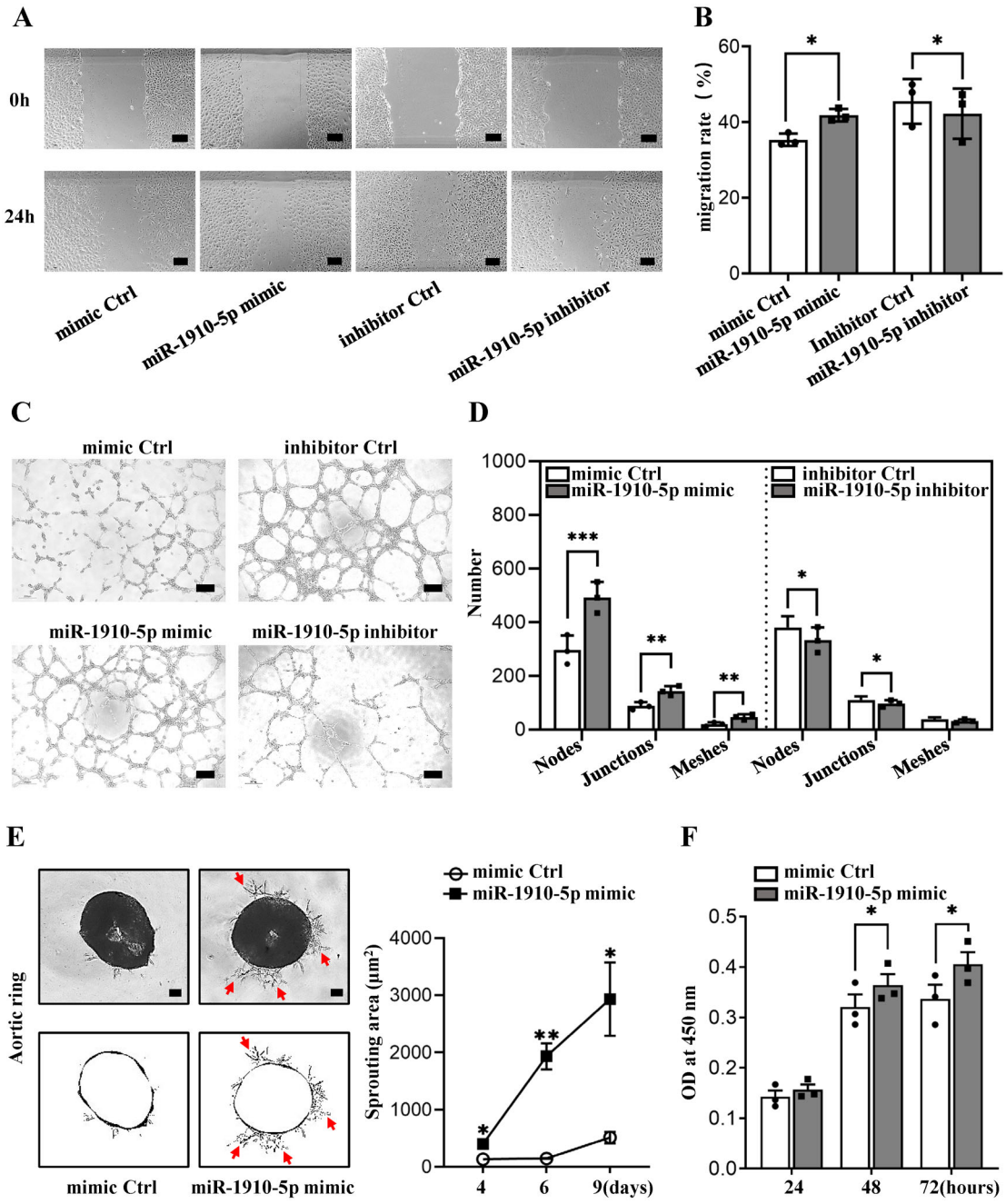

Figure 6. miR-1910-5p promoted HUVEC migration, tube formation, proliferation and increased angiogenesis in aortic rings. (**A**, **B**) Representative images and quantitative analysis of the wound healing assay. Scale bar, 100 μm. (**C**, **D**) Representative images and quantitative analysis of tube formation characterized the number of nodes, junctions, and meshes. Scale bar, 200 μm. (**E**) Mice aortic rings were transfected with the miR-1910-5p mimic or mimic control and cultured for 9 days. Representative images (*top*) and quantification of the microvascular sprouting area (*bottom*) from the mimic and mimic control groups. *Arrowheads* indicate microvascular sprouts. Scale bar, 200 μm. (**F**) CCK-8 assay results showed that miR-1910-5p mimic-treated HUVECs had higher levels of proliferative activity. Data are presented as the means ± SD ($n = 3$). *$P < 0.05$, **$P < 0.01$, ***$P < 0.001$. The Student *t*-test was used for comparison.

miR-1910-5p Mimic Decreases MMRN2 Expression and Causes Significant Extracellular Junctional Defects In Vitro

To further confirm the regulatory effect of miR-1910-5p on the expression of MMRN2, Western blotting assays also indicated that the miR-1910-5p mimic significantly suppressed the expression level of MMRN2, whereas the miR-1910-5p inhibitor significantly increased the MMRN2 expression level in HCE-T cells (Figs. 7F, G). The relative intensities of MMRN2 were quantified by densitometry and normalized to β-tubulin levels. Taken together, these data suggest that MMRN2 expression depends on miR-1910-5p, which directly targets the 3′-UTR of MMRN2.

In addition, we further investigated whether miR-1910-5p affects MMRN2 expressing in HUVECs, we assessed MMRN2 expression in HUVECs incubated with the CM of WT and CXCR4-KO cells treated with miR-1910-5p mimic and

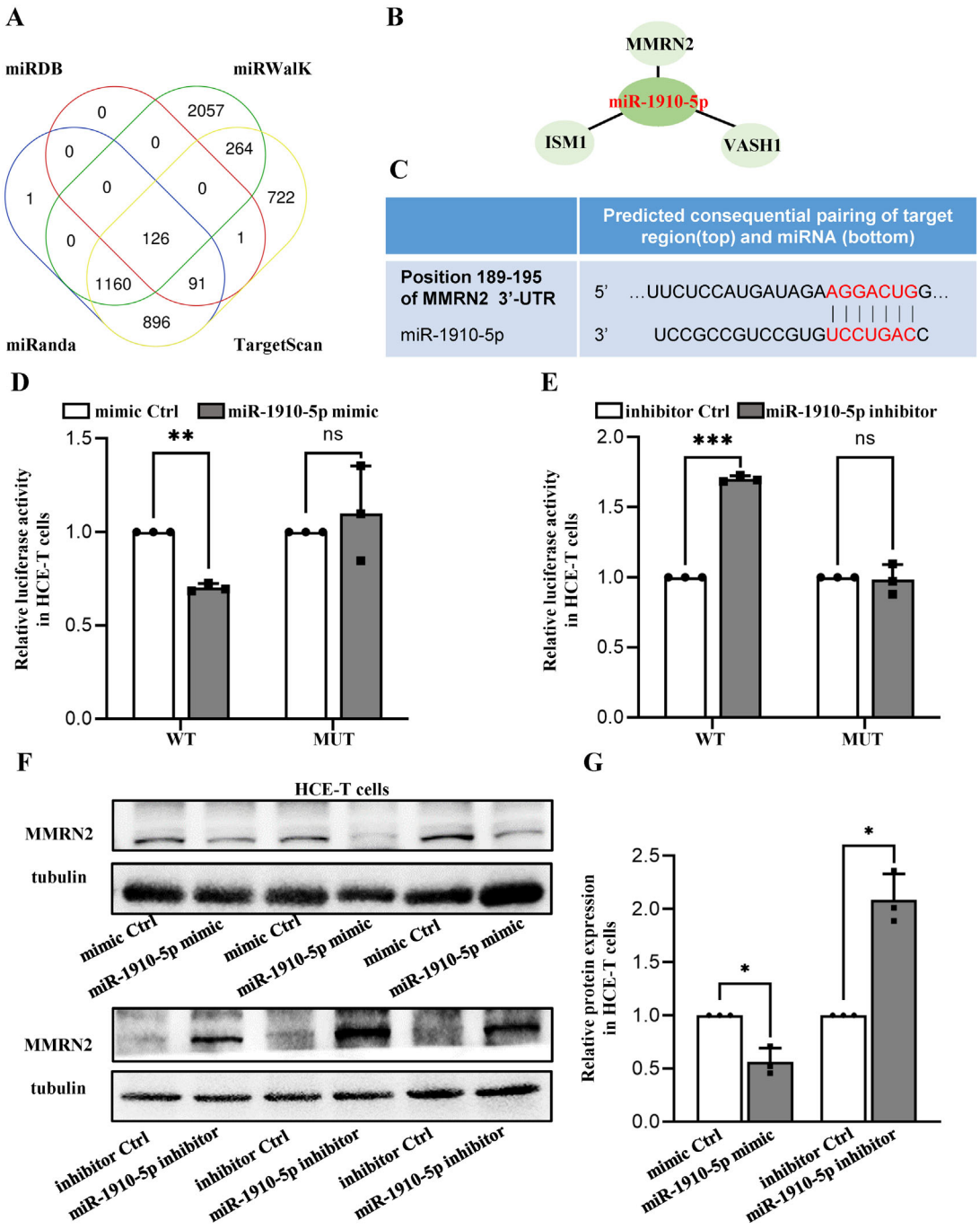

Figure 7. miR–1910–5p acted as a novel upstream regulator of MMRN2 by directly targeting its 3′-UTR. (**A**) Venn diagram of predicted miR-1910-5p targets by four different prediction algorithms (miRWalK, miRDB, TargetScan, and miRanda). Each labeled circle represents one prediction algorithm with the number of its predicted genes, and the number listed in overlapping circles is simultaneously predicted by different algorithms. (**B**) Bioinformatics prediction by the Database for Annotation, Visualization and Integrated Discovery online database of 3 target genes (VASH1, ISM1, and MMRN2) of miR-1910-5p that appear to be related to antiangiogenic function. (**C**) Sequences of miR-1910-5p and the potential miR-1910-5p-binding sites at the 3′-UTR of MMRN2. The seed sequence is marked in red. (**D**, **E**) A WT and mutant 3′-UTR-MMRN2 luciferase reporter and miR-1910-5p mimic (**D**) or inhibitor (**E**) were cotransfected into HCE-T cells, and luciferase activities were assessed. (**F**, **G**) Western blotting assay showed that the miR-1910-5p mimic could downregulate MMRN2 expression and that the miR-1910-5p inhibitor could upregulate MMRN2 expression in HCE-T cells. Data are presented as the means ± SD ($n = 3$). *$P < 0.05$, **$P < 0.01$, ***$P < 0.001$. The Student t-test was used for comparison.

control. As shown in Figure 8A, two bands were observed in Western blot assay. According to the molecular weight, the second bands were target of MMRN2. After calculating the band signal, our data indicated that the miR-1910-5p mimic decreased the expression of MMRN2 in HUVECs treated with both WT and CXCR4-KO HCE-T cell supernatant. The average ratio of MMRN2 to β-tubulin in control-treated cultures was defined as 1.0. The immunofluorescence assay also

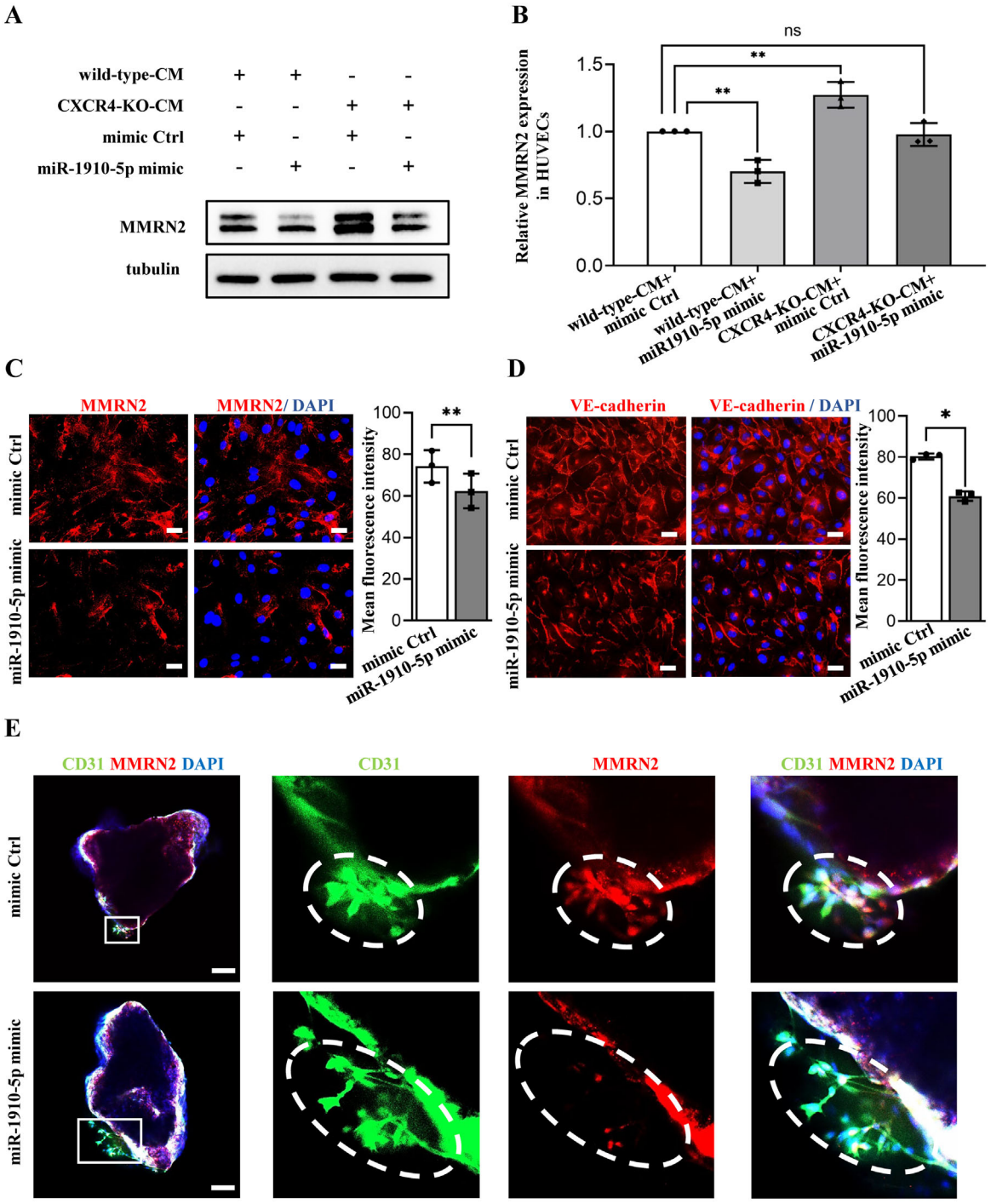

Figure 8. miR-1910-5p mimic decreases MMRN2 expressing and causes significant extracellular junctional defects in vitro. (**A**, **B**) Western blot analysis of MMRN2 protein expression in HUVECs incubated with CM from CXCR4-KO or WT HCE-T cells cotreated with miR-1910-5p-mimic or mimic control. (**C**) Representative images show the expression of MMRN2 following after with miR-1910-5p mimic and mimic control in HUVECs. Histogram showing that the miR-1910-5p mimic decreased the mean fluorescence intensity of MMRN2 compared with the mimic control group in HUVECs. (**D**) Representative images show the expression of VE-cadherin after transfection with the miR-1910-5p mimic in HUVECs. Histogram showing that the miR-1910-5p mimic decreased the mean fluorescence intensity of VE-cadherin compared with the mimic control group in HUVECs. Scale bars, 50 µm. (**E**) Representative pictures of the immunofluorescent staining of aortic rings. Endothelial sprouts were stained with CD31 (*green*) and MMRN2 (*red*), nuclei were stained with DAPI (*blue*), and merged pictures are shown. Scale bar, 200 µm. Data are presented as the means ± SD ($n = 3$). *$P < 0.05$, **$P < 0.01$. The Student *t*-test was used for comparison.

indicated that the protein expression of MMRN2 was down-regulated in HUVECs treated with miR-1910-5p mimics (Fig. 8C). Moreover, MMRN2, a protein deposited along blood vessels that maintains vascular homeostasis, is involved in vascular stability and permeability through extracellular junctions. In parallel, VE-cadherin, the adherens

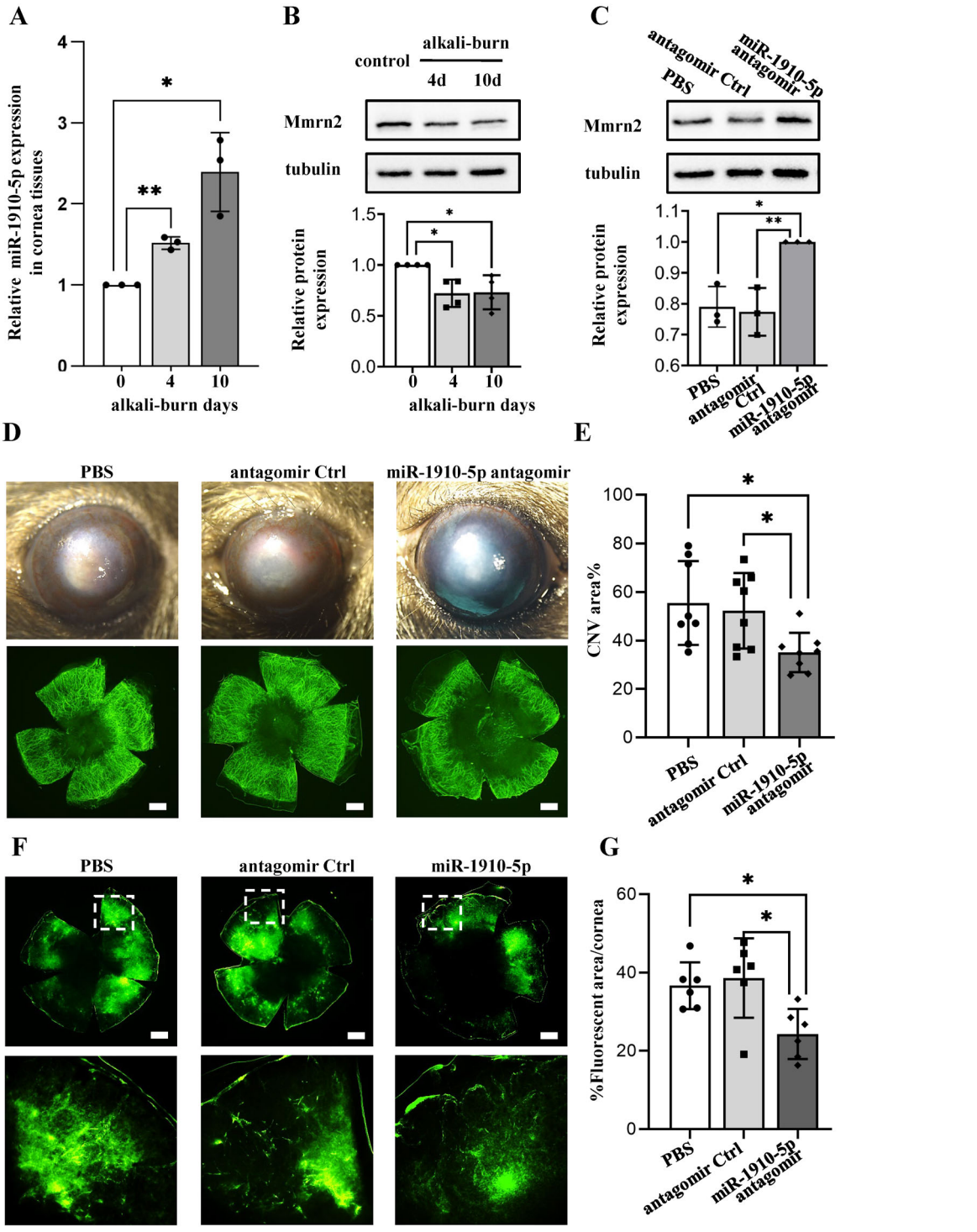

Figure 9. miR-1910-5p antagomir reverses EC junctional defects and decreases vascular leakage by increasing Mmrn2, and inhibits CNV in an alkali-burned murine model. (**A**) The qPCR analysis of miR-1910-5p in the corneas from the alkali-burned model at 4 and 10 days after injury compared with untreated corneas. (**B**) The protein expression of Mmrn2 was significantly downregulated in injured corneas at 4 and 10 days after alkali burn. (**C**) Western blotting analysis showed that the levels of Mmrn2 expression were significantly higher after miR-1910-5p antagomir treatment in alkali-burned corneas (n ≥ 3). (**D**) In vivo downregulation of miR-1910-5p attenuates CNV in a murine model of alkali injury. Representative images of corneal and CNV (green, CD31) with subconjunctival injection of PBS, antagomir control, and miR-1910-5p antagomir at 10 days after alkali burn. Scar bars, 200 µm. (**E**) CNV was quantified by measuring the neovascular area in the cornea and expressed as a percent of the total corneal area ($n = 8$). (**F**) Increased leakage of FITC-dextran (2000 kDa) through corneal neovessels after subconjunctival injection of PBS, antagomir control and miR-1910-5p antagomir at 10 days after alkali burn. Scale bars, 200 µm. (**G**) Corneal vessel leakage was quantified by measuring the fluorescence area in the cornea and expressed as a percent of the total corneal area ($n = 6$). Data are presented as the means ± SD, $^{*}P < 0.05$, $^{**}P < 0.01$. The Student *t*-test and one-way ANOVA were performed for comparison between two groups and multiple groups, respectively.

Investigative Ophthalmology & Visual Science

junction molecule, plays a key role in the maintenance of vascular integrity and permeability characteristics.[30] Accordingly, as shown in Figure 8D, the miR-1910-5p mimic also led to junction disruption of HUVECs stained with VE-cadherin. In parallel, we performed immunofluorescence staining for two additional critical proteins to further evaluate the junctional morphology. zonula occludens protein-1 is the tight junction protein, and β-catenin is a linker protein of junction integral membrane protein, which are known to be associated with vascular permeability.[31–33] Our results demonstrate that the expression of these two proteins is downregulated in the miR-1910 mimic group compared with the control, further indicating a potential decrease in the vascular permeability (Supplementary Figure S5). Furthermore, the expression of MMRN2 was confirmed in the aortic rings by inflorescence staining after transfection with the miR-1910-5p mimic and control. MMRN2-positive sprouting new vessels were found and were particularly abundant in the control group, but not in the mimic group (dashed ring, Fig. 8E). Therefore, miR-1910-5p directly targets MMRN2 and causes extracellular junctional defects in vascular ECs.

miR-1910-5p Antagomir Reverses EC Junctional Defects and Decreases Vascular Leakage by Increasing Mmrn2, and Inhibits CNV in an Alkali-burned Murine Model

Finally, we used a murine model of alkali burn-induced CNV to verify miR-1910-5p function in vivo. Although most miRNA targets are well-conserved in mammalian mRNAs, a similar miRNA sequence from the mouse source was not found in the publicly available database.[34] Therefore, we first detected whether miR-1910-5p is expressed in C57 mice. The relative expression levels in multiple organ tissues are presented in the Supplementary Materials. miR-1910-5p was confirmed to be specifically expressed in eyeballs (Supplementary Table S5). As anticipated, miR-1910-5p continued to increase with the extension of time in alkali-burned corneal tissues compared with the control group (Fig. 9A). The expression of Mmrn2 was also significantly downregulated at the protein level in alkali-burned corneas compared with that in the normal controls. The relative intensities of Mmrn2 were quantified by densitometry and normalized to β-tubulin levels (Fig. 9B).

Moreover, we administered a subconjunctival injection of miR-1910-5p antagomir, antagomir control, and PBS. Western blotting analysis revealed that Mmrn2 expression in corneal tissues was significantly higher after subconjunctival injection of the miR-1910-5p antagomir than in the antagomir control and PBS groups. The relative intensities of Mmrn2 were quantified by densitometry and normalized to β-tubulin levels (Fig. 9C). Fluorescence staining of CD31 indicated that the area of CNV in the miR-1910-5p antagomir-injected group was remarkably diminished compared with that of the miR-1910-5p antagomir control-injected and PBS-injected groups on day 10 after alkali burning (Figs. 9D–E). In addition, intravenous injection of FITC–dextran was performed to assay vascular leakage. As shown in Figures 9F and G, miR-1910-5p antagomir decreased vascular leakage in alkali-burned corneal tissues compared with the antagomir control and PBS groups. Collectively, these data further confirm that miR-1910-5p/MMRN2 is involved in CNV by effecting vascular stability and permeability in vivo.

Discussion

In this study, our data confirmed that CXCR4 was silenced in normal, healthy corneas, whereas it was remarkably upregulated in corneal tissues of patients with CNV (Fig. 1), which clinically demonstrated that CXCR4 plays an important role in CNV. Similarly, our previous study found that CXCR4 expression dramatically increased in alkali burn-induced CNV.[10] On the one hand, CXCR4 is essential for the recruitment of bone marrow–derived circulating EPCs in CNV.[4] Moreover, many studies have also demonstrated that CXCR4 plays a essential role in the homing of stem and progenitor cells in the bone marrow and modulates their mobilization into peripheral blood and tissues in response to injury.[35] On the other hand, CXCR4 antagonists have been demonstrated to be useful in inhibiting CNV in animal experiments. For example, subconjunctival injection of the CXCR4 antagonist plerixafor significantly alleviates CNV induced by alkali burns, as reported by Peng et al.[36] Specific blockade of CXCR4 with a neutralizing antibody has been proven to inhibit CNV progression.[37]

Moreover, our data indicated that CXCR4 promotes angiogenesis by affecting secreted materials from damaged corneal epithelial cells. The supernatant from hypoxia-treated HCE-T cells, which highly express CXCR4, increased HUVEC migration and tube formation in vitro (Supplementary Fig. S4). Conversely, the proangiogenic effect was alleviated after CXCR4 knockout in HCE-T cells (Fig. 3). Therefore, constituents of the supernatant from hypoxia-treated HCE-T cells might be changed after CXCR4 knockout. MiRNAs are abundant in different cells and as extracellular circulating miRNAs,[38] which play an important role in signal transduction pathways by regulating the translation and stability of target transcripts by being released into body fluids.[39] Some reports have indicated that miRNAs seem to target approximately 60% of the genes of humans and other mammals.[40,41] Therefore, in this study, we focused on the alteration of miRNAs induced by CXCR4 knockout.

Furthermore, a strength of this study is the discovery that miR-1910-5p plays a crucial role in CXCR4-mediated CNV by miRNA sequencing, bioinformatics analysis and gene interference. After searching PubMed, there were only several papers reporting the expression profile of miR-1910-5p. Kalaimani et al.[23] reported that miR-1910-5p was significantly upregulated in an enriched human corneal epithelial stem cell population in comparison to differentiated central corneal epithelial cells by small RNA sequencing. In tumor development, miR-1910-5p was highly expressed in locally advanced head and neck squamous cell carcinoma.[26] For its detailed biofunction, only two studies suggested contrary effects on damage stimulation. Ayaz and Dinç[24] indicated that H_2O_2 increased miR-1910-5p concentrations in ARPE-19 cells. However, the study by Mao and Wu[25] showed that miR-1910-5p was downregulated in extracellular vesicles in RPE cells treated with oxidized low-density lipoprotein. There are no papers reporting miR-1910-5p biofunction in vascularization and other diseases.

In our study, we found that miR-1910-5p was significantly higher in hypoxia-treated HCE-T cells and its supernatant of than normoxia-treated cells (Fig. 4F). Subsequently, miR-1910-5p function was confirmed both in vitro and in vivo. The miR-1910-5p mimic had an extremely proangiogenic effect (Fig. 6). Moreover, our data demonstrated that miR-1910-5p was significantly upregulated in the neovascularized corneas of mice. The therapeutic role of miR-1910-5p

Investigative Ophthalmology & Visual Science

in CNV was also confirmed in vivo by subconjunctival injection of the miR-1910-5p antagomir (Figs. 9D, E). Thus, our study provides strong evidence to support the idea that miR-1910-5p is involved in CNV.

Finally, the elucidation of the miR-1910-5p target downstream genes demonstrated that impairing vascular permeability might be responsible for CXCR4-mediated CNV through both in vitro and in vivo assays. MMRN2 was confirmed as a downstream target gene of miR-1910-5p (Figs. 7, 8, and 9). MMRN2 is an extracellular matrix glycoprotein and member of the elastin microfibril interface-located proteins.[42] Previous studies demonstrated that it can interfere with tumor angiogenesis and growth, serves as a TGF-β antagonist, and interferes with the VEGF-A/VEGFR2 pathway.[43,44] MMRN2 plays an important role in pathological vascularization of the choroid, revealing new possibilities for therapeutic intervention in neovascular AMD.[45] More important, two recent studies further elucidated the mechanism in detail. Fejza et al.[46] reported that MMRN2 is also deposited in juxtaposition between ECs and pericytes as a homeostatic molecule deposited in the later stages of vessel formation and is required to maintain vascular stability. A study by Pellicani et al.[31] further indicated that MMRN2 is a key molecule required to maintain vascular stability. Mmrn2$^{-/-}$ mice displayed cell junctional defects, impaired pericyte recruitment, more collapsed vessels, and increased vascular leakage.[31] Moreover, in our study, overexpression of miR-1910-5p led to a significantly decreased expression of MMRN2 and VE-cadherin in HUVECs compared with those in cells treated with the control (Fig. 8). In vivo data also showed that the miR-1910-5p antagomir decreased vascular leakage in alkali-burned corneal tissues compared with the control and PBS groups (Figs. 9F, G). These results strongly support that excessive miR-1910-5p suppresses the expression of MMRN2 and impairs proper vessel stabilization.

In addition, there are some limitations to the present study. First, of note, bone marrow-derived circulating EPCs play a key role in vasculogenesis in response to injury.[4] Therefore, we hypothesize that miR-1910-5p decreases MMRN2, subsequently attenuating vascular stability and increasing vascular leakage, which stimulates EPC migration to the damaged corneal limbus. We tried to find EPC migration but failed. We speculate that we did not choose the correct time point for the in vivo experiment. Second, CXCR4 is usually located on the cell surface and in the cytoplasm.[47] Our data show that CXCR4 translocates from the cytoplasm to the nucleus under hypoxia treatment (Figs. 5D, G). Thus, CXCR4 enters the nucleus and might perform an upstream transcriptional activation role to regulate the expression of miR-1910-5p. However, we did not provide direct evidence to support it. We analyzed the upstream sequence (−2589 bp to +529 bp) of C16orf74 (the host gene of miR-1910-5p) by luciferase reporter assays. Unfortunately, −2589 bp to +529 bp is not its promoter region. The determination of the promoter of miRNA is relatively difficult.[48,49] Further studies are required to validate that the specific promoter region of CXCR4 directly binds to the promoter of miR-1910-5p for its transcription. Of course, there is another possibility, namely, that CXCR4 may indirectly regulate miR-1910-5p transcription. In addition, in Figures 7F and 8A, there are two bands in the samples from human cells with a rabbit polyclonal antibody from Cloud-Clone Corp (PAF593Hu01, specific to human). According to the molecular weight, the second bands were target of MMRN2. Therefore, MMRN2 might be modified by phosphorylation or methylation. However, there is only one band in mouse sample when we used a rabbit polyclonal antibody from Cloud-Clone Corp (PAF593Mu01, specific to mouse) in a Western blot assay (Figs. 9B, C). Thus, we speculate that there is a potential possibility induced by nonspecific cross-reactions.

In summary, to our knowledge, our study reveals a novel mechanism of CXCR4-mediated CNV both in vitro and in vivo. MiR-1910-5p is an intrinsic promoter of pathologic ocular angiogenesis through suppression of MMRN2. CXCR4/miR-1910-5p/MMRN2 plays a significant role in the early stage of CNV by impairing vascular stability and permeability. Thus, this study not only reveals a CXCR4-mediated mechanism, but also suggests that miR-1910-5p could be a promising therapeutic target for CNV in clinical treatment in the future.

Acknowledgments

The authors thank Guangzhou Huaxiang Medical Biotechnology Co., Ltd., for bioinformatics support.

Supported by the National Natural Science Foundation [grant number: 82101134] and Guangzhou Science Technology and Innovation Commission [grant number: 201803010091].

Disclosure: **X. Wang**, None; **Z. Cui**, None; **X. Chen**, None; **Q. Luo**, None; **Z. Jiang**, None; **X. Liu**, None; **Y. Huang**, None; **J. Jiang**, None; **S. Chen**, None; **J. Qiu**, None; **Y. Li**, None; **K. Yu**, None; **J. Zhuang**, None

References

1. Nicholas MP, Mysore N. Corneal neovascularization. *Exp Eye Res.* 2021;202:108363.
2. Gupta D, Illingworth C. Treatments for corneal neovascularization: A review. *Cornea.* 2011;30(8):927–938.
3. Roshandel D, Eslani M, Baradaran-Rafii A, et al. Current and emerging therapies for corneal neovascularization. *Ocular Surf.* 2018;16(4):398–414.
4. Takahashi T, Kalka C, Masuda H, et al. Ischemia- and cytokine-induced mobilization of bone marrow-derived endothelial progenitor cells for neovascularization. *Nat Med.* 1999;5(4):434–438.
5. Claesson-Welsh L. Vascular permeability–the essentials. *Upsala J Med Sci.* 2015;120(3):135–43.
6. Teicher BA, Fricker SP. CXCL12 (SDF-1)/CXCR4 pathway in cancer. *Clin Cancer Res.* 2010;16(11):2927–2931.
7. Petit I, Jin D, Rafii S. The SDF-1-CXCR4 signaling pathway: A molecular hub modulating neo-angiogenesis. *Trends Immunol.* 2007;28(7):299–307.
8. Walter DH, Haendeler J, Reinhold J, et al. Impaired CXCR4 signaling contributes to the reduced neovascularization capacity of endothelial progenitor cells from patients with coronary artery disease. *Circ Res.* 2005;97(11):1142–1151.
9. Omori K, Nagata N, Kurata K, et al. Inhibition of stromal cell-derived factor-1α/CXCR4 signaling restores the blood-retina barrier in pericyte-deficient mouse retinas. *JCI Insight.* 2018;3(23):e120706.
10. Wu Y, Xu Z, Yang Y, et al. Tetramethylpyrazine (TMP) ameliorates corneal neovascularization via regulating cell infiltration into cornea after alkali burn. *Biomed Pharmacother.* 2019;109:1041–1051.
11. Tang M, Yang Y, Yu J, et al. Tetramethylpyrazine in a murine alkali-burn model blocks NFκB/NRF-1/CXCR4-signaling induced corneal neovascularization. *Invest Ophthalmol Vis Sci.* 2018;59(5):2133–2141.

12. de Nigris F, Crudele V, Giovane A, et al. CXCR4/YY1 inhibition impairs VEGF network and angiogenesis during malignancy. *Proc Natl Acad Sci USA.* 2010;107(32):14484–14489.
13. Caporali A, Emanueli C. MicroRNA regulation in angiogenesis. *Vasc Pharmacol.* 2011;55(4):79–86.
14. Tiwari A, Mukherjee B, Dixit M. MicroRNA key to angiogenesis regulation: miRNA biology and therapy. *Current Cancer Drug Targets.* 2018;18(3):266–277.
15. Rupaimoole R, Slack FJ. MicroRNA therapeutics: Towards a new era for the management of cancer and other diseases. *Nat Rev Drug Discov.* 2017;16(3):203–222.
16. O'Brien J, Hayder H, Zayed Y, Peng C. Overview of microRNA biogenesis, mechanisms of actions, and circulation. *Front Endocrinol.* 2018;9:402.
17. Zhang Y, Zhang T, Ma X, Zou J. Subconjunctival injection of antagomir-21 alleviates corneal neovascularization in a mouse model of alkali-burned cornea. *Oncotarget.* 2017;8(7):11797–11808.
18. Lu Y, Tai PWL, Ai J, et al. Transcriptome profiling of neovascularized corneas reveals miR-204 as a multi-target biotherapy deliverable by rAAVs. *Mol Ther Nucleic Acids.* 2018;10:349–360.
19. Zong R, Zhou T, Lin Z, et al. Down-regulation of microRNA-184 is associated with corneal neovascularization. *Invest Ophthalmol Vis Sci.* 2016;57(3):1398–1407.
20. Wang H-F, Dong Z-Y, Yan L, et al. The N-terminal polypeptide derived from vMIP-II exerts its antitumor activity in human breast cancer through CXCR4/miR-7-5p/Skp2 pathway. *J Cell Physiol.* 2020;235(12):9474–986.
21. Klein S, Abraham M, Bulvik B, et al. CXCR4 promotes neuroblastoma growth and therapeutic resistance through miR-15a/16-1-mediated ERK and BCL2/cyclin D1 pathways. *Cancer Res.* 2018;78(6):1471–1483.
22. Anderson C, Zhou Q, Wang S. An alkali-burn injury model of corneal neovascularization in the mouse. *J Vis Exp.* 2014;(86):51159.
23. Kalaimani L, Devarajan B, Subramanian U, et al. MicroRNA profiling of highly enriched human corneal epithelial stem cells by small RNA sequencing. *Sci Rep.* 2020;10(1):7418.
24. Ayaz L, Dinç E. Evaluation of microRNA responses in ARPE-19 cells against the oxidative stress. *Cutaneous Ocul Toxicol.* 2018;37(2):121–126.
25. Mao K, Wu X. Microarray analysis of small extracellular vesicle-derived miRNAs involved in oxidative stress of RPE cells. *Oxid Med Cell Longev* 2020;2020:7658921.
26. Panvongsa W, Siripoon T, Worakitchanon W, et al. Plasma extracellular vesicle microRNA-491-5p as diagnostic and prognostic marker for head and neck squamous cell carcinoma. *Cancer Sci.* 2021;112(10):4257–4269.
27. Cabioglu N, Sahin A, Doucet M, et al. Chemokine receptor CXCR4 expression in breast cancer as a potential predictive marker of isolated tumor cells in bone marrow. *Clinical & Experimental Metastasis.* 2005;22(1):39–46.
28. Yoshitake N, Fukui H, Yamagishi H, et al. Expression of SDF-1 alpha and nuclear CXCR4 predicts lymph node metastasis in colorectal cancer. *Br J Cancer.* 2008;98(10):1682–1689.
29. He X, Wei Q, Zhang X, et al. Immunohistochemical expression of CXCR4 in thyroid carcinomas and thyroid benign lesions. *Pathol Res Pract.* 2010;206(10):712–715.
30. Giannotta M, Trani M, Dejana E. VE-cadherin and endothelial adherens junctions: Active guardians of vascular integrity. *Dev Cell.* 2013;26(5):441–454.
31. Pellicani R, Poletto E, Andreuzzi E, et al. Multimerin-2 maintains vascular stability and permeability. *Matrix Biol* 2020;87:11–25.
32. Dejana E, Tournier-Lasserve E, Weinstein BM. The control of vascular integrity by endothelial cell junctions: Molecular basis and pathological implications. *Dev Cell.* 2009;16(2):209–221.
33. González-Mariscal L, Domínguez-Calderón A, Raya-Sandino A, Ortega-Olvera JM, Vargas-Sierra O, Martínez-Revollar G. Tight junctions and the regulation of gene expression. *Semin Cell Dev Biol.* 2014;36:213–223.
34. Fromm B, Billipp T, Peck LE, et al. A uniform system for the annotation of vertebrate microRNA genes and the evolution of the human microRNAome. *Annu Rev Genet.* 2015;49:213–242.
35. Döring Y, Pawig L, Weber C, Noels H. The CXCL12/CXCR4 chemokine ligand/receptor axis in cardiovascular disease. *Front Physiol.* 2014;5:212.
36. Peng L-H, Shen W, Yong W, Lu L, Liu L. Effects of AMD3100 subconjunctival injection on alkali burn induced corneal neovascularization in mice. *Int J Ophthalmol.* 2011;4(1):44–48.
37. Lopez MJ, Seyed-Razavi Y, Jamali A, Harris DL, Hamrah P. The chemokine receptor CXCR4 mediates recruitment of CD11c+ conventional dendritic cells into the inflamed murine cornea. *Invest Ophthalmol Vis Sci.* 2018;59(13):5671–5681.
38. Krol J, Loedige I, Filipowicz W. The widespread regulation of microRNA biogenesis, function and decay. *Nat Rev Genet.* 2010;11(9):597–610.
39. Mori MA, Ludwig RG, Garcia-Martin R, Brandão BB, Kahn CR. Extracellular miRNAs: From biomarkers to mediators of physiology and disease. *Cell Metab.* 2019;30(4):656–673.
40. Lewis BP, Burge CB, Bartel DP. Conserved seed pairing, often flanked by adenosines, indicates that thousands of human genes are microRNA targets. *Cell.* 2005;120(1):15–20.
41. Friedman RC, Farh KK-H, Burge CB, Bartel DP. Most mammalian mRNAs are conserved targets of microRNAs. *Genome Res.* 2009;19(1):92–105.
42. Colombatti A, Spessotto P, Doliana R, Mongiat M, Bressan GM, Esposito G. The EMILIN/Multimerin family. *Front Immunol.* 2011;2:93.
43. Lorenzon E, Colladel R, Andreuzzi E, et al. MULTIMERIN2 impairs tumor angiogenesis and growth by interfering with VEGF-A/VEGFR2 pathway. *Oncogene.* 2012;31(26):3136–3147.
44. Colladel R, Pellicani R, Andreuzzi E, et al. MULTIMERIN2 binds VEGF-A primarily via the carbohydrate chains exerting an angiostatic function and impairing tumor growth. *Oncotarget.* 2016;7(2):2022–2037.
45. Tosi GM, Neri G, Barbera S, et al. The binding of CD93 to multimerin-2 promotes choroidal neovascularization. *Invest Ophthalmol Vis Sci.* 2020;61(8):30.
46. Fejza A, Poletto E, Carobolante G, et al. Multimerin-2 orchestrates the cross-talk between endothelial cells and pericytes: A mechanism to maintain vascular stability. *Matrix Biol Plus.* 2021;11:100068.
47. Bianchi ME, Mezzapelle R. The chemokine receptor CXCR4 in cell proliferation and tissue regeneration. *Front Immunol.* 2020;11:2109.
48. Fujita S, Iba H. Putative promoter regions of miRNA genes involved in evolutionarily conserved regulatory systems among vertebrates. *Bioinformatics.* 2008;24(3):303–308.
49. Zhao Y, Wang F, Chen S, Wan J, Wang G. Methods of microRNA promoter prediction and transcription factor mediated regulatory network. *BioMed Res Int* 2017;2017:7049406.

Investigative Ophthalmology & Visual Science